Title	Quantitative assessment of the comparative nanoparticle-uptake efficiency of a range of cell lines
Authors(s)	dos Santos, Tiago; Varela, Juan; Lynch, Iseult; Dawson, Kenneth A.; Salvati, Anna
Publication date	2011-12-02
Publication information	Small, 7 (23): 3341-3349
Publisher	Wiley
Link to online version	http://dx.doi.org/10.1002/smll.201101076
Item record/more information	http://hdl.handle.net/10197/3533
Publisher's statement	This is the author's version of the following article: Tiago dos Santos, Juan Varela, Iseult Lynch, Kenneth Dawson (2011) "Quantitative Assessment of the Comparative Nanoparticle-Uptake Efficiency of a Range of Cell Lines" SMALL nano micro, 7 : 3341-3349 which has been published in final form at http://dx.doi.org/10.1002/smll.201101076
Publisher's version (DOI)	10.1002/smll.201101076

Submitted to small NANO MICRO

Quantitative assessment of the comparative nanoparticle-uptake efficiency of a range of cell lines

Tiago dos Santos, Juan Varela, Iseult Lynch, Anna Salvati, Kenneth A. Dawson**

Centre for BioNano Interactions, School of Chemistry and Chemical Biology, University College Dublin, Belfield, Dublin 4, Ireland

*Kenneth A. Dawson (Kenneth.A.Dawson@cbni.ucd.ie); Tiago dos Santos (Tiago.Santos@cbni.ucd.ie)

Centre for BioNano Interactions, School of Chemistry and Chemical Biology, University College Dublin, Belfield, Dublin 4, Ireland

Phone: +353 (0)1 716 6928; Fax: +353 (0)1 716 2415

Keywords: Nanoparticles, Cellular uptake, size effects, Particle tracking, Flow cytometry

Abstract

Interest continues to grow in the possibility of understanding the mechanism(s) of nanoparticle-cell interactions. At present there is little knowledge, and essentially no understanding, of the relevant length and time scales for nanoparticle-intracellular entry, and localization within cells, and the cell-specificity of nanoparticle uptake and localisation. We have investigated here the effect of particle size on the *in vitro* intracellular uptake of model fluorescent carboxyl-modified polystyrene nanoparticles in various cell lines commonly used for uptake studies. A range of micro- and nanoparticles of defined sizes (40 nm to 2 μm) were

incubated with a series of cell types, including HeLa and A549 epithelial cells, 1321N1 astrocytes, HCMEC D3 endothelial cells and murine RAW 264.7 macrophages. Techniques such as confocal microscopy and flow cytometry were used to study particle uptake and sub-cellular localisation, making significant efforts to ensure reproducibility in a semi-quantitative approach. The results indicated that internalization of (nano)particles is highly size dependent for all cell lines studied and that the kinetics of uptake for the same nanoparticle varies in the different cell types. Interestingly, even cells non specialized for phagocytosis were able to internalize the larger nanoparticles. Intracellular uptake of all sizes of (nano)particles was observed to be the highest in RAW 264.7 cells (a specialized phagocytic cell line) and the lowest in the HeLa cells. Results suggests that (nano)particle uptake might not follow commonly defined size limits for uptake processes and highlights the variability of uptake kinetics for the same material in different cell types. These conclusions have important implications for the assessment of the safety of nanomaterials and potential biomedical applications of nanoparticles.

1. Introduction

Understanding and manipulation of biological processes on the nanoscale level is a strong driving force behind the development of nanotechnology. The fundamental interactions of nanoscale objects with living matter will play a central role in the realization of nanomedicine. This new field is expected to create innovative tools for various biomedical applications, not only in drug delivery and gene therapy, but also in molecular imaging, biomarkers and biosensors[1]. The fact that nanoparticles (NPs) exist in the same size domain as proteins (typical sizes of 5 nm) makes them suitable for bio-tagging or labelling, allowing researchers to "spy" on the cellular machinery without (in principle) perturbing it,[2, 3] while at the same time NPs offer a way to engage via specific interactions with the cell and its

machinery. However, this unique potential access of NPs to the cellular machinery could lead to new and unintended consequences and biological impacts from nanomaterials never intended for contact with humans, and it is this concern that has spawned the field of nanosafety assessment.

It is commonly believed that smaller than about 200 nm particles may enter unspecialized cells with ease, less than 35 nm particles sometimes enter the nucleus[2], and less than 30 nm particles may be transported into the central nervous system[4]. While small molecules such as hydrophobic dyes (and small drugs) can freely diffuse and partition inside cells according to their physico-chemical properties, nanoscale objects have a size appropriate to engage with the cellular machinery, and are thereby trafficked by the cell via energy dependent pathways, in much the same manner as biomolecules and proteins[5-12]. This has raised legitimate concerns about their safety[13] .

Phagocytic cells such as macrophages are able to engulf and digest cellular debris and pathogens, and as such are essential to vertebrate animal's defense mechanisms.[14] Their phagocytic and microbicidal activities are essential for maintaining organs, such as lungs and intestine, in a clean and sterile state[15-18]. It is well known that macrophages are capable of removing large particles from the blood, once recognized by the immune system.[19] A major challenge in the development of drug delivery motifs is to be able to intravenously target and delivery polymeric NPs without their clearance from the systemic circulation by blood monocytes and cells of the phagocyte system, which are specialized for uptake and removal of larger particles[20, 21].

Cellular uptake studies have demonstrated that several other cell lines, including cells not specialized for phagocytosis are also able to uptake NPs with different internalization

capacities[22-24]. Nevertheless, uptake of different sizes of NPs has not been widely or systematically investigated in different cellular barriers and using cells from different organs. Several works can be found in the literature where carboxylated polystyrene nanoparticles of different sizes have been used as model nanoparticles to investigate uptake properties and efficiency of internalisation. For example, Rejman and colleagues suggest that non-phagocytic B16 cells show an upper size limit of 200 nm for internalization negatively polystyrene NPs, using clathrin mediated endocytosis[25]. Another example suggests that clathrin does not mediate the uptake of negatively charged polystyrene NPs in HeLa cells[26]. In our previous work, we have used carboxylated polystyrene of different sizes to investigate the effect of heat inactivation of the serum on the uptake in A549 cells[27]. A549 cells were also used to quantify the efficiency of internalisation and the intracellular location of silica nanoparticle of different sizes[28]. HeLa cells are commonly used as a model cell line to study nanoparticle uptake, not only in the case of polystyrene nanoparticles, but also for other nanoparticle types, such as fullerenes, which were internalized via the clathrin-mediated endocytosis pathway,[29] and gold nanoparticles of different size and shape[30, 31]. Some of the results available in literature, for studies using nanoparticles and cell types similar to those applied here, are given in Table S1, as a reference. These examples reveal how difficult it is to derive conclusions regarding how general or pervasive NP uptake mechanisms are across cell lines, and to understand how different particle sizes, particle compositions, or particle shapes can trigger different cellular interactions, and how these depend on and/or vary with the cell type. Nevertheless, a striking output from the literature and the examples included in Table S1 is that it is evident that NPs (in some cases even up to 500 nm) seem to enter very different cell types with ease, and it is hard to find references where NPs do not enter the cell (with the exceptions of some bacteria and plant cells, where the cell wall prevents uptake[32-38]).

In previous work, we have established ways to ensure quantitative reproducibility of uptake and sub-cellular accumulation of NPs into cells. There we found NP uptake to be energy dependent, with NPs accumulating in the lysosomes and no signs of export and degradation from this location[28, 39]. Here, prior to any assessment of the details of the uptake mechanisms exploited by the NPs to enter cells, we seek to expand these initial studies to a panel of NPs of different sizes, and to a series of different cell types, in order to investigate whether nanoparticle uptake efficiency (internalised load), and uptake kinetics are similar in a wider context, and thereby to determine whether some general conclusions regarding particle *in vitro* uptake can be drawn.

For this purpose, we have investigated the uptake of model negatively charged carboxylated-modified polystyrene (PS-COOH) NPs with very different sizes, from sizes comparable to typical endocytic cargoes (40 nm, 100 nm, 200 nm, 500 nm) to micron sized objects (1 μm, 2 μm) such as those recognized by specialized cells of the immune system. In order to try to identify general behavior for NP uptake across all of the investigated particle sizes, the study has been performed *in vitro* using a panel of different cell types, mainly epithelial, but with different tissues of origin, representing the primary exposure routes for NPs from the external environment. These cell types are also used routinely in the literature to study biological processes and to screen for nanotoxicity and they included: HeLa (tumoral epithelial cells from cervix, commonly used to study cell biology of uptake mechanisms[31, 40, 41]), A549 (endothelial cells from lung carcinoma, widely applied in toxicity studies for lung exposure scenarios[42]), 1321N1 (glial cells from brain astrocytoma, which are a good model for impact in the central nervous system, besides neurons[43, 44]), HcMEC D3 (brain endothelial cells, which are used as an *in vitro* model of the human blood brain barrier,[45] and thus to investigate the capacity of NPs to cross barriers[37]), and RAW 264.7 (murine macrophages, classically

applied to study specialized phagocytic mechanisms[46, 47]). It is noteworthy that despite the fact that these cells have different characteristics, such as different sizes, different doubling times (see Figure S1 in the supplementary material), or different preferential growth media, every effort has been made in this study to ensure that they were treated in the same way in all steps from cell preparation (cell number and confluence degree) to exposure to nanoparticles (nanoparticle batch and dose, cell growth medium and serum protein composition). In this way we could compare the results across the different cell types and derive conclusions on the cell-specific differences in uptake.

2- Results and discussion

Carboxylated-modified polystyrene nanoparticles (PS-COOH) were chosen as model particles for the study of uptake and interaction in different cell lines for a variety of reasons, including their established non-toxicity when exposed to cells[44]. They are commercially available in different sizes, are fluorescently labeled and are well characterized, and moreover they form stable monodisperse dispersions, including in cell media with serum proteins. We have also confirmed (see below) that the samples used here show minimal dye leakage under the cellular conditions used[39]. Combined, these properties make them as a good model particle, which ensures that cells are interrogated with stable samples of homogeneous characteristics, thereby avoiding misinterpretations which could arise in the case of NP aggregation or polydispersity (wide distribution of different sizes), or from dye leakage confounding the uptake data.

Nanoparticle characterization in both PBS and complete cell growth medium (complete MEM) is shown in Table 1. For all the NPs, the hydrodynamic size measured in complete MEM was higher than the values obtained in PBS, although all samples are still monodisperse

and there is no evidence of particle aggregation. This is due to protein adsorption on the surface of the NPs[48, 49], which also resulted in a slightly higher polydispersity index (PDI). Moreover, the zeta potential values in cMEM were closer to 0 than those in PBS, because of the screening effect of the protein corona covering the NPs[27]. This suggests that the stabilisation mechanism switches from electrostatic to steric due to the protein corona surrounding the particles. These results are in agreement with previous literature[27].

A poorly appreciated problem in NP uptake studies such as those reported here is the potential presence of residual dye from the particle labeling process that is released from NPs in a biological medium, and in particular within the cell[50]. Such contamination could lead to misinterpretation of particle uptake and localisation results. Thus, gel electrophoresis under appropriate conditions (Figure S2) has been used as a tool to confirm the absence of any labile dye for all the particles used in this study. The results indicated that the majority of the dye was associated with the NPs, and thus that these NPs are suitable for quantitative cellular uptake studies and also for tracking by fluorescence microscopy.

Great effort was made to expose cells to NPs at equal cell numbers and at comparable cell confluence degrees, in order to compare results obtained with populations at similar cell densities. This was achieved by seeding the same number of cells and waiting 24h before performing the experiment, to allow proper cell adhesion.

Although the different cell lines were grown in different media to meet their optimal cell growth requirements and ensure that the cells were not stressed prior to the experiments, exposure to nanoparticles was performed for all cell types in complete MEM medium as follows: the cells were seeded at same cell density in the medium required for each cell type, supplemented with fetal bovine serum from a common batch, and after 24h, the medium was replaced by the NP dispersion, which was prepared for all cell types in complete MEM. None

of the investigated cell lines showed any changes in phenotype or evidence of cell death when grown in the cMEM containing NPs, at least for the duration of the experiment. After exposure to NPs, a washing procedure was optimized and implemented to determine the number of PBS washes necessary to accurately remove surface bound polystyrene NPs from the cells (Figure S3). This analysis has been optimized for HeLa and A549 cells and was then applied to all cell lines used in the study (fluorescence imaging further confirmed the optimisation for all cells and NP sizes).

In order to understand the level of NP internalization in the different cell lines, the data were normalised for the fluorescence of a single nanoparticle of each size. The cells were exposed to the same mass of nanoparticles for all sizes, thus the starting dispersions contained different particle numbers and different total fluorescence intensity, as measured by fluorescence spectroscopy and shown in Figure S4.

The fluorescence intensity per particle for the different particle sizes is given in Table S2, and was calculated by dividing the fluorescence emission of the starting suspension (measured in Figure S4) by the number of NPs in the applied mass (see Supporting Information for details). For this calculation, the hydrodynamic diameter in PBS as determined by DLS (datashown in Table 1) was used. All flow cytometry data were normalised by the values in Table S2 for the corresponding NP size. This normalisation allows direct comparison of NP accumulation results for the different particle sizes and for a given NP size across the different cell types. Additionally, to rule out any influence from the normalisation method on the data, normalisation using the fluorescence intensity of the total applied NP mass was also calculated (see Supplementary information): this was obtained by dividing the mean cell fluorescence intensity (obtained from flow cytometry) by the fluorescence emission of the starting NP suspensions (measured in Figure S4).

The particle concentration used in this work (20 µg/ml) did not induce any evident cellular toxicity due to uptake, for all particle sizes, despite the particle numbers differing by a factor of four, as shown in Table S2. No significant cell loss was detectable by flow cytometry for cells exposed for 24h to the different NPs, in comparison with untreated cells under the same conditions. This is in agreement with results already available in literature for similar nanoparticles[39, 44].

Individual intracellular fluorescence intensity was measured via flow cytometry and averages were taken over large numbers (typically 10,000-30,000) of fixed cells to produce a time-resolved averaged intracellular fluorescence curve. Figure 1 shows typical cell fluorescence distributions, obtained from HeLa cells treated for 24h with the different particle sizes (40 nm, 100 nm, 200 nm, 500 nm) at same mass concentration (20 µg/ml) in cMEM. The same experiment was performed for all the cell lines in this study and in all cases, similar distributions were observed, as shown in Supplementary Figure S5. For small NP sizes, the fluorescence distribution over the cell population was narrow, suggesting a homogenous uptake for all cells in the sample. Thus, the averaged mean cell fluorescence intensities, normalised as detailed above, were calculated and are shown in Figure 2. (The normalisation by the fluorescence intensity of the total applied mass is also shown in Figure S6 for comparison).

Increasing the size of the NPs resulted in the cell fluorescence distribution becoming broader, since, as discussed further below, for cells exposed to larger particles, small differences in the numbers of internalised particles between cells resulted in noticeably different total fluorescence intensity per cell. Because of this effect, the full fluorescence distribution is shown (see Figure 3) for cells treated with 1µm nanoparticles.

A first observation from our results is that uptake of NPs is highly particle size dependent, meaning that, applying the same particle mass in all cases (thus different NP numbers), with increased NP size the uptake dramatically decreased, even for macrophages which are designed for uptake of particles > 200 nm. When comparing results across the different cell types for a given NP size, a first important observation is the overall higher internalization capacity of macrophages compared with the other tested cell lines, and especially compared to the non-specialised HcMEC D3 cells, not only for the larger particles, as expected from the specialised phagocytic mechanisms used by this type of cell, but even more apparently for the smaller particle sizes. This strong difference in uptake efficiency could indicate that different uptake mechanisms are used in the two different cell lines for these NPs. It is noteworthy that HcMEC D3 cells have the ability to take on polarized properties that can lead to different uptake rates. In fact studies where HcMEC D3 cells were used as a human blood brain barrier cell model shows that NPs are internalized differently to when the cells are not polarized[37, 51].

In the case of the smaller PS-COOH NPs, we can exclude saturation of the cells at the applied dose as the source of the difference in internalisation across cell types, since dose dependence experiments have shown that 20 µg/ml is a concentration far from uptake saturation (as shown in previous work) [27, 37, 39, 44].

With increasing NP size (200 nm, 500 nm), the difference of uptake across the different cell lines started to decrease, suggesting a similar uptake mechanism for particles of this intermediate size range in the different cell types. Other researchers have already suggested a similar size-dependency in cellular uptake of different particles[52, 53]. (A summary of some of the results available in the literature for the uptake of PS-COOH NP of different sizes and in cell lines such as those used here is given in Table S1).

Figure 3A shows the cell fluorescence distributions after exposure to 1µm microparticles, and compares the uptake efficiency across the different cell lines tested (single nanoparticles were excluded, together with cell debris, by gating the forward scattering as explained in the Methods section). These results are extremely interesting, and to our knowledge have never been reported in the past. As described previously, due to the large size of these particles, a small variation in the number of internalised NPs per cell, *n*, gives rise to a strong difference in the acquired cellular fluorescence intensity, thus making it possible to discriminate and quantify the exact number of internalised NPs in the different cell sub-populations (n=0-4). This is shown in Figure 3A, where we can resolve fluorescence peaks at distinct intensities, depending on the number (*n*) of particles internalized by each sub-population of cells.

The settings in the flow cytometry instrument were kept constant for all cell lines, so that the mean values of each of the peaks (indicated by the gates P1 to P4) are constant across the investigated cell types, with the only variable being the amount of cells which internalized the different numbers, *n*, of NPs. Figure 3B shows the percentage of cells as a function of the number of internalized NPs, *n*, indicating the higher capacity of HCMEC D3 and RAW 264.7 cells to internalize a higher amount ($n > 3$) of particles per cell (60 and 76% respectively), in contrast with HeLa and A549 cells (5 and 17% of cells had n>3 particles per cell). Similar results could be observed by analyzing the percentage of cells with zero particles taken up, where HeLa and A549 cells showed the highest proportion of cells with no particles, indicating their comparative inability to internalise 1 µm sized particles.

With the 1µm diameter particles, the probability of having cells with no particles internalized after the given exposure time was 74 and 52% for HeLa and A549 cells respectively, compared with 9 and 3% for HCMEC D3 and RAW 264.7 cells, respectively. Identical results were observed for 2 µm particles (Figure S7), and more details can be seen in Table S3. An important result shown by these data is that the uptake rate for the larger NPs (1 and 2

μm particles) is much slower, compared to that of the smaller particle sizes. Thus, even after 24h of exposure to the 1 or 2 μm particles, cells with no NPs internalised were found. On the contrary, for the smaller particle sizes, even after short incubation times, all cells in the population showed NP uptake and a single peak of cell fluorescence intensity was obtained covering the full cell population. As explained above, differences in the internalised NPs numbers between cells are more difficult to discriminate for the smaller particle sizes. Nevertheless, it is surprising to see that these large NPs can also enter cells that are not specialised for phagocytosis. Similar results were reported in literature for HeLa cells[52]. This could be explained by residual phagocytic capability even for these cells, but could also be a reflection of novel interactions and uptake pathways induced by particles of this size engaging with the cellular machinery, although further studies are needed to fully clarify the uptake mechanisms.

Confocal microscopy images for cells treated with these larger particles can help to discriminate between internalized and externally adsorbed particles, and can also provide additional information regarding the intracellular location of the particle-associated fluorescent signals. Figure 4 shows the uptake of 1μm diameter PS-COOH particless after 24h of exposure, for all the cell lines used in this study. The enlarged detail in the lower corner shows an orthogonal view of a Z-stack performed on individual cells, providing sufficient evidence that particles were located within the cell boundaries.

Corroborating the flow cytometry results discussed above, a higher capacity of internalization by RAW264.7 and HCMEC D3 cells was observed also with confocal microscopy, when compared with 1321N1, A549 and HeLa cells, again showing the strong dependence of NP uptake not only on particle size, but also on the cell type.

Regarding the final localization of the NPs, Lesniak *et al.* have shown that these same 40nm and 100nm PS-COOH accumulated in the lysosomes in A549 cells[27]. Similar results were

observed here for all of the investigated cell lines. As shown in Figure S8, after 4 hours of incubation, confocal images indicated that a high number of the 40 nm particles are already accumulated in the lysosomal compartments, confirming that these particles follow an acidic endo-lysosomal pathway[54]. Similarly, we found particle localisation in the lysosomes for the other particle sizes investigated (as an example, see Figure S9 for HCMEC D3 cells, where NPs colocalised with green Lysotracker). However, further studies are required to confirm this result for the 1 and 2 µm PS-COOH particles.

In order to further investigate the differences in NP uptake across the different cell lines, kinetic profiles of NP uptake were obtained and are shown, for the first 4h of exposure, in Figure 5 for the 40 nm (A) and 200 nm (B) NPs in all five cell types studied (the insets show the same profiles over 24h, which are also shown in Supplementary Figure S10).

At 24h, these kinetic profiles showed an apparent decrease in the uptake rate for all of the cells and both particle sizes. This is related to the cell doubling time and cell division phenomena, rather than to saturation[28, 39]. Upon cell division, the load of internalised NPs is split between the daughter cells, thus diluting the total average cell fluorescence intensity, giving rise to an apparent saturation of uptake. The cell doubling times are in the range of 15h-24h, depending on the cell line (see Figure S1). The higher uptake rate observed previously for RAW 264.7 cells was confirmed already at early exposure times, which again suggests that these cell are not only specialised in the uptake of larger particles, but also seem to have higher avidity for smaller particles (higher rate of uptake). This can be further confirmed by calculating the slopes (over the first 4h of uptake) from the time resolved curves obtained with the RAW 264.7 cells, and comparing them with the slopes obtained from the other cell lines (Table S4). In the case of the 40 nm PS-COOH NPs, RAW 264.7 cells had a

slope (kinetics of uptake) which was 8, 18, 20 and 56 times higher than that observed for HCMEC D3, 1321N1, A549 and HeLa cells, respectively, while for the 200 nm particles, the fold increase of the RAW 264.7 cells relative to the HCMEC D3, 1321N1, A549 and HeLa cells was 11, 42, 67, 182, respectively.

3- Conclusions

A quantitative *in vitro* study of cellular uptake of different sizes of fluorescently-labeled PS-COOH NPs with different sizes, ranging from 40 nm to 2 μm has been performed in five different cell lines. All NPs entered all cell types (although with quite different uptake rates), including the larger sizes, even in those cells not specialized for phagocytosis. The uptake of PS-COOH NPs was highly size dependent for all cell lines, and was driven by their capacity for particle internalization. Particule uptake kinetics showed a higher internalization rate in the RAW 264.7 macrophages, not only for the large particle sizes, as expected by the specialized nature of these cells, but also for the smaller particle sizes. These results clearly point out that for a given NP very different doses can be internalized by different cell types, and that the rate of particle uptake changes strongly with the NP size, with the larger sizes getting inside the cells much more slowly than the smaller ones.

4- Experimental Section

Cell culture

Human glial astrocytoma 1321N1cells (passage 2-10) were cultured at 37 ºC in 5% CO_2 in Dulbecco's Modified Eagle's Medium (DMEM) supplemented with 10% fetal bovine serum (FCS, Gibco) and 1% penicillin/streptomycin (Invitrogen Corp.).

Murine macrophage-like RAW 264.7 cells (passage 5-10) were cultured at 37 ºC in 5% CO_2 in Minimum Essential Medium (MEM, with additional L-Glutamine) supplemented with 10% Fetal Calf Serum (FCS, Gibco) and 1% penicillin/streptomycin (Invitrogen Corp.).

Human lung epithelium A549 cells (passage 1-30 after defrosting from liquid nitrogen; original batches at passage number 105 or 82) were cultured at 37 ºC in 5% CO_2 in Minimum Essential Medium (MEM, with additional L-Glutamine) supplemented with 10% Fetal Calf Serum (FCS, Gibco), 1% penicillin/streptomycin (Invitrogen Corp.), and 1% MEM non-essential amino acids (HyClone).

Human cervix epithelium HeLa cells (passage 5-10) were cultured at 37 ºC in 5% CO_2 in Minimum Essential Medium (MEM, with additional L-Glutamine) supplemented with 10% Fetal Calf Serum (FCS, Gibco) and 1% penicillin/streptomycin (Invitrogen Corp.) .

Human brain capillary endothelial HCMEC D3 cells were obtained from Florence Miller, B.B. Weksler (INSERM, France). HCMEC D3 cells (passage 9-21) were cultured at 37 ºC in 5% CO_2 in EBM-2 medium supplemented with hFGF (LONZA), Genatmicin sulfate/amphotericin B (LONZA), Hepes 1mM Buffer (LONZA), fetal calf serum (FCS, Gibco), and hydrocortisone.

It is important to note that although different mediums were used to culture the different cell lines, the same FCS was used in all cases, in order to ensure maximum biological reproducibility across all cell lines. All cell lines were confirmed to be mycoplasma negative using the mycoAlert kit (Lonza Inc. Allendale, NJ) and were tested monthly.

Nanoparticles

Texas Red dye-loaded (Excitation/Emission wavelengths: 580/605) PS-COOH NPs (Fluospheres® size kit, Invitrogen) were used without further modification or purification. Particle sizes used in this work were 40 nm, 100 nm, 200 nm, 500 nm, 1000 nm (1 µm), 2000

nm (2 µm). All stock solutions were stored at 4 ^{0}C, and used within 1 year of receiving, in order to ensure their stability.

NP dispersions were prepared by diluting the concentrated stock solutions into complete medium (cMEM) at room temperature, immediately prior to the experiments on cells, with an identical time delay between diluting and introducing particle dispersions to the cells for all experiments. The medium was kept at room temperature and not pre-warmed to 37 °C to ensure better NP dispersion quality. Before sampling, NPs were vigorously mixed as recommended by the company.

The mean size and surface charge of the different sized NPs were determined using a photon correlation spectrophotometer (Malvern Zetasizer Nano ZS). Measurements were performed at 25^{0}C in PBS and in complete MEM. The particle size distribution and zeta potential data are presented in Table 1.

Protocols for nanoparticle and cell handling for quantitative uptake kinetics studies

During this work, considerable effort was applied to determine the optimal conditions needed to ensure that quantitatively reproducible experiments could be performed. Several different parameters were considered and studied, including optimal cell numbers for seeding, washing protocols to ensure that surface-adherent NPs were removed, procedures for fixing the cells, and the optimal timing of all of these procedures.

SDS PAGE

SDS Polyacrylamide Gel Electrophoresis (PAGE) gels (4% stacking gel and 10% resolving gel) were used to estimate the ratio of fluorescence due to NPs and labile dye (Figure S2). NPs (2.0 mg/ml) were diluted 1:1 with loading buffer (10% mercaptoethanol, and 20% glycerol in Tris/HCl 25 nM pH 6.9, with 10% SDS), and loaded into the stacking gel at a

concentration of 20 µg/ml. Gels were run at 120 mV for 45 minutes. Pictures were acquired using a Fujifilm Intelligent dark box LAS-3000, exciting the gels with a blue light at 460 nm and emission was recorded with a 515 nm filter. Images were taken at 2 second exposure times.

Flow cytometry analysis

2.5 x 10^5 cells were seeded in individual 60 mm tissue culture dishes (Greiner Bio-one), and incubated for 24h prior to addition of particles to allow proper adhesion (the cell number didn´t change significantly in these first 24h). After 24 hours, the medium was replaced by the medium containing NPs. Cells were incubated with NPs for a certain time, depending on the experiment, and then the medium was removed and discarded. Samples were washed thrice with DPBS and harvested with 0.05% trypsin/EDTA 1x. Although RAW 264.7 are usually circulatory, seeding does not affect their functionality.[55] However, trypsin wasn't used because it would damage the cells[56], and so these cells were harvested from the plate by pipetting vigorously. Cell pellets were then fixed with 4% formalin solution neutral buffered (Sigma) for 20 minutes and re-suspended with constant volumes of DPBS before cell-associated fluorescence (10,000 - 40,000 cells per sample) was detected using a Coulter EPICS XL-MCL reader (Brennan and company) and/or a CyAn ADP (DAKO) flow cytometer. Forward and side scattering dot plots were used to discriminate cellular debris and, in the case of the 1 and 2 µm particle sizes, which were large enough to be detected, to exclude residual nanoparticles external to cells from the analysis. In all the cases, to ensure reproducibility, the waiting time between sample preparation and measurement was kept constant, at a minimum of 1.5 hour, to ensure complete stability of the sample. Strong modifications of the side scattering, forward scattering and fluorescence intensities were detected in the 1st hour, after which all these parameters were more constant with time, but

still changing slightly. Samples were stored in darkness at 4^0C before measurement. The results are reported as the mean of the distribution of cell fluorescence intensity, averaged between 2 independent replica. Error bars are the standard deviation between the replica. The full time curves were performed at least 3 times. Flow cytometry was carried out in Flow Cytometry Core Facility of the University College Dublin, Conway Institute

Fluorescence microscopy

For confocal microscopy, 4.0 x 10^4 cells were seeded onto glass slides (Falcon, 4 well slides) and incubated for 24h prior to addition of particles. The cell number was set to ensure a cell density comparable to the flow cytometry experiments and, in order to keep all parameters affecting the experiment constant, the same protocols were used as for exposure to particles, sample preparation and cell fixation. Thus, particle dispersions were prepared at room temperature just before addition to the cells and, after particle exposure for 1 hour, medium was removed and all samples were washed thrice with DPBS, fixed with 4% formalin solution neutral buffered, the nucleus stained with 4',6-diamidino-2-phenylindole (DAPI blue), and the F-actin stained with fluorescein-phaloidin (Invitrogen Corp.), before analysis.

A confocal microscope (Carl Zeiss LSM 510 UVMETA, Thornwood, NY) was used to capture images of the intracellular environment and the sub-cellular localization of the fluorescent NPs. For multi-color microscopy, samples were excited with 364 nm (blue channel), 488 nm (green channel), and 543 nm (red channel) laser lines, and images were captured by multi-tracking to avoid bleed-through between the fluorophores. To achieve the necessary signal to noise ratio, while obtaining the thinnest possible optical slices, the pinhole diameters were set to less than 1 airy unit. After adjustment of the pinholes of both lasers to obtain the same optical slices, the optimal optical section that fulfilled our criteria was in the range 0.7 - 0.8 µm at 63X. The gain and offset for the different channels were kept constant

along the full series of experiments for each cell type (although the different cell types were optimized individually) in order to allow qualitative comparison of the cell fluorescence intensities following exposure to the different particle sizes.

Immunostaining and co-localization

For the immunostaining study, after exposure to NPs and fixation as described above, cells were permeabilised with 0.1% Saponin (Sigma Aldrich) for 5 minutes before staining the actin filaments using Texas-red or Fluorescein- phalloidin (Invitrogen Corp.) for 20min. In the case of co-localization studies, after the fixation and permeabilization steps described above, cells were blocked with 10% Bovine Serum Albumin in PBS Tween for 30 minutes. Cells were then incubated with anti Lamp1 antibody (ABCAM) for 1 hour at room temperature, washed and finally incubated with Alexa488 conjugated secondary antibody for 1 hour (Molecular Probes). The cells were washed as before (3 times for 3 minutes each with 1x PBS) and then stained with DAPI for 5 minutes. The mounting medium was Mowiol (Calbiochem).

Lysotracker Green was also used to assess co-localization of NPs with lysosomes. Live cells were stained with 750 nM Lysotracker Green (Invitrogen) in growth medium for one hour at 37 ^{0}C and 5% CO_2. After organelle staining, the medium was replaced by fresh growth medium. Cells were then imaged with a confocal microscope in a live cell chamber at 37 ^{0}C and 5% CO_2.

Acknowledgements

This work was performed within the scope of an SFI RFP (CHP031, TdS) and the EU FP6 project NanoInteract (NMP4-CT-2006-033231, AS, IL). Additional financial support from FP6 IST project SIGHT (IST-2005-033700, JV), the SFI SRC BioNanoInteract (07 SRC

B1155, AS) and SFI RFP (MTR2425, JV) is also acknowledged. The ESF Research Networking Programme EpitopeMap is also gratefully acknowledged for funding an exchange trip (TdS). Access to, and use of, instrumentation of the UCD Conway Flow Cytometry Core Facility and the UCD Conway Imaging Core Facility is gratefully acknowledged.

REFERENCES

1. Allianz, O. *Small sizes that matter: Opportunities and risks of Nanotechnologies*; 2004.
2. Gu, Y. J.; Cheng, J. P.; Lin, C. C.; Lam, Y. W.; Cheng, S. H.; Wong, W. T., Nuclear penetration of surface functionalized gold nanoparticles. *Toxicology and Applied Pharmacology* **2009,** *237* (2), 196-204.
3. Prina-Mello, A.; Whelan, A. M.; Atzberger, A.; McCarthy, J. E.; Byrne, F.; Davies, G. L.; Coey, J. M. D.; Volkov, Y.; Gun'ko, Y. K., Comparative Flow Cytometric Analysis of Immunofunctionalized Nanowire and Nanoparticle Signatures. *Small 6* (2), 247-255.
4. Oberdorster, G.; Sharp, Z.; Atudorei, V.; Elder, A.; Gelein, R.; Kreyling, W.; Cox, C., Translocation of inhaled ultrafine particles to the brain. *Inhalation Toxicology* **2004,** *16* (6-7), 437-445.
5. Conner, S. D.; Schmid, S. L., Regulated portals of entry into the cell. *Nature* **2003,** *422* (6927), 37-44.
6. Watson, P.; Jones, A. T.; Stephens, D. J., Intracellular trafficking pathways and drug delivery: fluorescence imaging of living and fixed cells. *Advanced Drug Delivery Reviews* **2005,** *57* (1), 43-61.
7. Jones, A. T.; Gumbleton, M.; Duncan, R., Understanding endocytic pathways and intracellular trafficking: a prerequisite for effective design of advanced drug delivery systems. *Advanced Drug Delivery Reviews* **2003,** *55* (11), 1353-1357.
8. Mayor, S.; Pagano, R. E., Pathways of clathrin-independent endocytosis. *Nature Reviews Molecular Cell Biology* **2007,** *8* (8), 603-612.
9. Panyam, J.; Labhasetwar, V., Dynamics of endocytosis and exocytosis of poly(D,L-lactide-co-glycolide) nanoparticles in vascular smooth muscle cells. *Pharmaceutical Research* **2003,** *20* (2), 212-220.
10. Kaksonen, M.; Toret, C. P.; Drubin, D. G., Harnessing actin dynamics for clathrin-mediated endocytosis. *Nature Reviews Molecular Cell Biology* **2006,** *7* (6), 404-414.
11. Luhmann, T.; Rimann, M.; Bitterman, A. G.; Hall, H., Cellular uptake and intracellular pathways of PLL-g-PEG-DNA nanoparticles. *Bioconjugate Chemistry* **2008,** *19* (9), 1907-1916.
12. Mailander, V.; Landfester, K., Interaction of Nanoparticles with Cells. *Biomacromolecules* **2009,** *10* (9), 2379-2400.

13. Stern, S. T.; McNeil, S. E., Nanotechnology safety concerns revisited. *Toxicological Sciences* **2008,** *101* (1), 4-21.
14. Kauffman, H. F., Innate immune responses to environmental allergens. *Clinical Reviews in Allergy & Immunology* **2006,** *30* (2), 129-140.
15. Seiler, P.; Aichele, P.; Odermatt, B.; Hengartner, H.; Zinkernagel, R. M.; Schwendener, R. A., Crucial role of marginal zone macrophages and marginal zone metallophils in the clearance of lymphocytic choriomeningitis virus infection. *European Journal of Immunology* **1997,** *27* (10), 2626-2633.
16. Geiser, M., Morphological aspects of particle uptake by lung phagocytes. *Microscopy Research and Technique* **2002,** *57* (6), 512-522.
17. Geiser, M.; Casaulta, M.; Kupferschmid, B.; Schulz, H.; Semirriler-Behinke, M.; Kreyling, W., The role of macrophages in the clearance of inhaled ultrafine titanium dioxide particles. *American Journal of Respiratory Cell and Molecular Biology* **2008,** *38* (3), 371-376.
18. Alexis, N. E.; Lay, J. C.; Zeman, K. L.; Geiser, M.; Kapp, N.; Bennett, W. D., In vivo particle uptake by airway macrophages in healthy volunteers. *American Journal of Respiratory Cell and Molecular Biology* **2006,** *34* (3), 305-313.
19. Warner, A. E.; Brain, J. D., Intravascular pulmonary macrophages - a novel cell removes particles from blood. *American Journal of Physiology* **1986,** *250* (4), R728-R732.
20. Chono, S.; Tanino, T.; Seki, T.; Morimoto, K., Efficient drug delivery to alveolar macrophages and lung epithelial lining fluid following pulmonary administration of liposomal ciprofloxacin in rats with pneumonia and estimation of its antibacterial effects. *Drug Development and Industrial Pharmacy* **2008,** *34* (10), 1090-1096.
21. Zahr, A. S.; Davis, C. A.; Pishko, M. V., Macrophage uptake of core-shell nanoparticles surface modified with poly(ethylene glycol). *Langmuir* **2006,** *22* (19), 8178-8185.
22. Yacobi, N. R.; DeMaio, L.; Xie, J. S.; Hamm-Alvarez, S. F.; Borok, Z.; Kim, K. J.; Crandall, E. D., Polystyrene nanoparticle trafficking across alveolar epithelium. *Nanomedicine-Nanotechnology Biology and Medicine* **2008,** *4* (2), 139-145.
23. Huang, M.; Ma, Z. S.; Khor, E.; Lim, L. Y., Uptake of FITC-chitosan nanoparticles by a549 cells. *Pharmaceutical Research* **2002,** *19* (10), 1488-1494.
24. Davda, J.; Labhasetwar, V., Characterization of nanoparticle uptake by endothelial cells. *International Journal of Pharmaceutics* **2002,** *233* (1-2), 51-59.
25. Rejman, J.; Oberle, V.; Zuhorn, I. S.; Hoekstra, D., Size-dependent internalization of particles via the pathways of clathrin-and caveolae-mediated endocytosis. *Biochemical Journal* **2004,** *377*, 159-169.
26. Dausend, J.; Musyanovych, A.; Dass, M.; Walther, P.; Schrezenmeier, H.; Landfester, K.; Mailander, V., Uptake Mechanism of Oppositely Charged Fluorescent Nanoparticles in HeLa Cells. *Macromolecular Bioscience* **2008,** *8* (12), 1135-1143.
27. Lesniak, A.; Campbell, A.; Monopoli, M. P.; Lynch, I.; Salvati, A.; Dawson, K. A., Serum heat inactivation affects protein corona composition and nanoparticle uptake. *Biomaterials* **2010,** *31* (36), 9511-9518
28. Shapero, K.; Fenaroli, F.; Lynch, I.; Cottell, D. C.; Salvati, A.; Dawson, K. A., Time and space resolved uptake study of silica nanoparticles by human cells. *Molecular Biosystems* **2011,** *7* (2), 371-378.
29. Li, W.; Chen, C. Y.; Ye, C.; Wei, T. T.; Zhao, Y. L.; Lao, F.; Chen, Z.; Meng, H.; Gao, Y. X.; Yuan, H.; Xing, G. M.; Zhao, F.; Chai, Z. F.; Zhang, X. J.; Yang, F. Y.; Han, D.; Tang, X. H.; Zhang, Y. G., The translocation of fullerenic nanoparticles into

lysosome via the pathway of clathrin-mediated endocytosis. *Nanotechnology* **2008,** *19* (14).

30. Chithrani, B. D.; Chan, W. C. W., Elucidating the mechanism of cellular uptake and removal of protein-coated gold nanoparticles of different sizes and shapes. *Nano Letters* **2007,** *7* (6), 1542-1550.
31. Chithrani, B. D.; Ghazani, A. A.; Chan, W. C. W., Determining the size and shape dependence of gold nanoparticle uptake into mammalian cells. *Nano Letters* **2006,** *6* (4), 662-668.
32. Macfie, S. M.; Welbourn, P. M., The Cell Wall as a Barrier to Uptake of Metal Ions in the Unicellular Green Alga <i>Chlamydomonas reinhardtii</i> (Chlorophyceae). *Archives of Environmental Contamination and Toxicology* **2000,** *39* (4), 413-419.
33. Eggeling, L.; Sahm, H., The cell wall barrier of Corynebacterium glutamicum and amino acid efflux. *Journal of Bioscience and Bioengineering* **2001,** *92* (3), 201-213.
34. De Lorenzo, G.; D'Ovidio, R.; Cervone, F., The role of Polygalacturonase-inhibiting proteins (PGips) in defense against pahtogenic fungi. *Annual Review of Phytopathology* **2001,** *39* (1), 313-335.
35. Baier, G.; Costa, C.; Zeller, A.; Baumann, D.; Sayer, C.; Araujo, P. H. H.; Mailander, V.; Musyanovych, A.; Landfester, K., BSA Adsorption on Differently Charged Polystyrene Nanoparticles using Isothermal Titration Calorimetry and the Influence on Cellular Uptake. *Macromolecular Bioscience 11* (5), 628-638.
36. Lunov, O.; Syrovets, T.; Loos, C.; Beil, J.; Delacher, M.; Tron, K.; Nienhaus, G. U.; Musyanovych, A.; MailaÌˆnder, V.; Landfester, K.; Simmet, T., Differential Uptake of Functionalized Polystyrene Nanoparticles by Human Macrophages and a Monocytic Cell Line. *Acs Nano 5* (3), 1657-1669.
37. Ragnaill, M. N.; Brown, M.; Ye, D.; Bramini, M.; Callanan, S.; Lynch, I.; Dawson, K. A., Internal benchmarking of a human blood-brain barrier cell model for screening of nanoparticle uptake and transcytosis. *European Journal of Pharmaceutics and Biopharmaceutics* **2011,** *77* (3), 360-367.
38. Zhang, Y.; Kohler, N.; Zhang, M., Surface modification of superparamagnetic magnetite nanoparticles and their intracellular uptake. *Biomaterials* **2002,** *23* (7), 1553-1561.
39. Salvati, A.; Aberg, C.; dos Santos, T.; Varela, J.; Pinto, P.; Lynch, I.; Dawson, K., Experimental and theoretical comparison of intracellular import of polymeric nanoparticles and small molecules: Towards models of Uptake Kinetics. *Nanomedicine: Nanotechnology, Biology and Medicine* **2011,** *in press*.
40. Osaki, F.; Kanamori, T.; Sando, S.; Sera, T.; Aoyama, Y., A quantum dot conjugated sugar ball and its cellular uptake on the size effects of endocytosis in the subviral region. *Journal of the American Chemical Society* **2004,** *126* (21), 6520-6521.
41. Lu, F.; Wu, S. H.; Hung, Y.; Mou, C. Y., Size Effect on Cell Uptake in Well-Suspended, Uniform Mesoporous Silica Nanoparticles. *Small* **2009,** *5* (12), 1408-1413.
42. Tahara, K.; Sakai, T.; Yamamoto, H.; Takeuchi, H.; Hirashima, N.; Kawashima, Y., Improved cellular uptake of chitosan-modi fled PLGA nanospheres by A549 cells. *International Journal of Pharmaceutics (Kidlington)* **2009,** *382* (1-2), 198-204.
43. Gann, H.; Glaspell, G.; Garrad, R.; Wanekaya, A.; Ghosh, K.; Cillessen, L.; Scholz, A.; Parker, B.; Warner, M.; Delong, R. K., Interaction of MnO and ZnO Nanomaterials with Biomedically Important Proteins and Cells. *Journal of Biomedical Nanotechnology* **2010,** *6* (1), 37-42.

44. Bexiga, M. G.; Varela, J. A.; Wang, F.; Fenaroli, F.; Salvati, A.; Lynch, I.; Simpson, J. C.; Dawson, K. A., Cationic nanoparticles induce caspase 3-, 7- and 9-mediated cytotoxicity in a human astrocytoma cell line. *Nanotoxicology 10.3109/17435390.2010.539713* (0).
45. Weksler, B. B.; Subileau, E. A.; Perriere, N.; Charneau, P.; Holloway, K.; Leveque, M.; Tricoire-Leignel, H.; Nicotra, A.; Bourdoulous, S.; Turowski, P.; Male, D. K.; Roux, F.; Greenwood, J.; Romero, I. A.; Couraud, P. O., Blood-brain barrier-specific properties of a human adult brain endothelial cell line. *Faseb Journal* **2005,** *19* (11), 1872-1874.
46. Lai, Y. R.; Chiang, P. C.; Blom, J. D.; Li, N.; Shevlin, K.; Brayman, T. G.; Hu, Y. D.; Selbo, J. G.; Hu, L. G., Comparison of in vitro nanoparticles uptake in various cell lines and in vivo pulmonary cellular transport in intratracheally dosed rat model. *Nanoscale Research Letters* **2008,** *3* (9), 321-329.
47. Wilhelm, C.; Gazeau, F.; Roger, J.; Pons, J. N.; Bacri, J. C., Interaction of anionic superparamagnetic nanoparticles with cells: Kinetic analyses of membrane adsorption and subsequent internalization. *Langmuir* **2002,** *18* (21), 8148-8155.
48. Lynch, I.; Salvat, i. A.; Mahon, E.; Baldelli Bombelli, F.; A. Dawson, K., Designer nanoparticles-protein coronas: specifying epitope conformation at the corona surface to pre-determine nanoparticles interactions with cellular machinery.
49. Walczyk, D.; Bombelli, F. B.; Monopoli, M. P.; Lynch, I.; Dawson, K. A., What the Cell "sees" in Bionanoscience. *Journal of the American Chemical Society* **2010,** *132* (16), 5761-5768.
50. Preston, R. A.; Murphy, R. F.; Jones, E. W., Apparent endocytosis of fluorescein isothiocyanate conjugated dextran by saccharomyces-cerevisiae reflects uptake of low-molecular-weight impurities, not dextran. *Journal of Cell Biology* **1987,** *105* (5), 1981-1987.
51. Vu, K.; Weksler, B.; Romero, I.; Couraud, P.-O.; Gelli, A., Immortalized Human Brain Endothelial Cell Line HCMEC/D3 as a Model of the Blood-Brain Barrier Facilitates In Vitro Studies of Central Nervous System Infection by Cryptococcus neoformans. *Eukaryotic Cell* **2009,** *8* (11), 1803-1807.
52. Gratton, S. E. A.; Ropp, P. A.; Pohlhaus, P. D.; Luft, J. C.; Madden, V. J.; Napier, M. E.; DeSimone, J. M., The effect of particle design on cellular internalization pathways. *Proceedings of the National Academy of Sciences* **2008,** *105* (33), 11613-11618.
53. Yin Win, K.; Feng, S.-S., Effects of particle size and surface coating on cellular uptake of polymeric nanoparticles for oral delivery of anticancer drugs. *Biomaterials* **2005,** *26* (15), 2713-2722.
54. Lai, S. K.; Hida, K.; Man, S. T.; Chen, C.; Machamer, C.; Schroer, T. A.; Hanes, J., Privileged delivery of polymer nanoparticles to the perinuclear region of live cells via a non-clathrin, non-degradative pathway. *Biomaterials* **2007,** *28* (18), 2876-2884.
55. Fraser, I.; Hughes, D.; Gordon, S., Divalent Cation-independent macrophage adhesion inhibited by monoclonal-antibody to murine scavenger receptor. *Nature* **1993,** *364* (6435), 343-345.
56. Allen, J. M.; Cook, G. M. W., A study of attachment phase of phagocytosis by murine macrophages. *Experimental Cell Research* **1970,** *59* (1), 105-116.

The table of contents entry

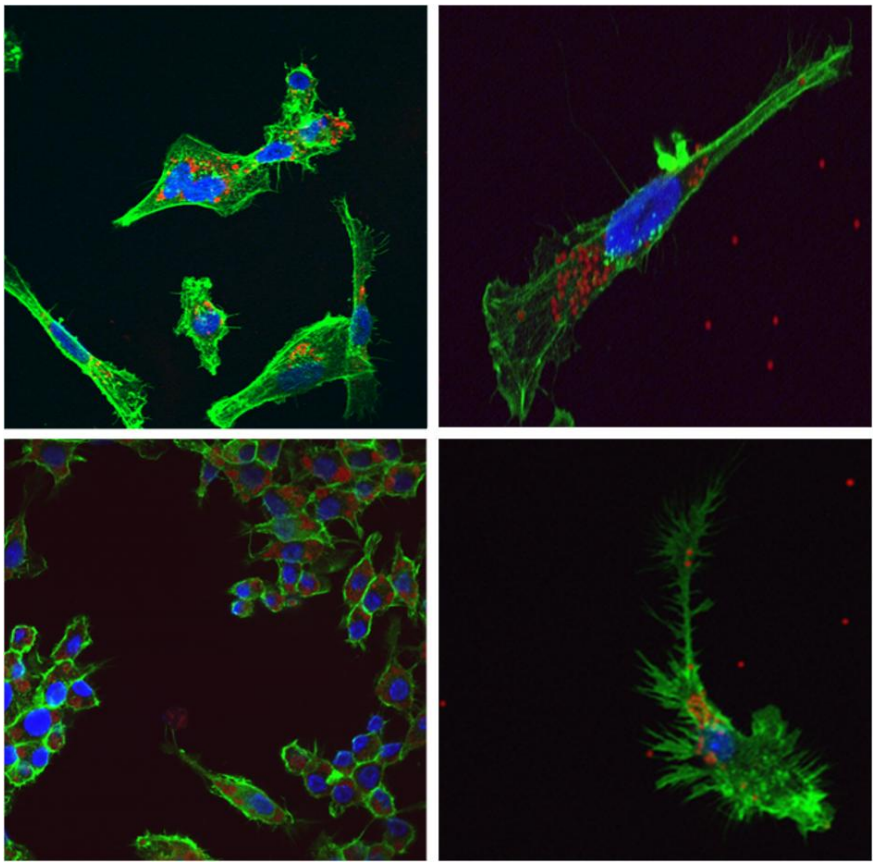

Comparative study of the uptake of Texas-red labeled carboxylate-modified polystyrene nanoparticles by a panel of cell lines. Shown here is uptake of 40 nm (left side) and 1000 nm (right side) particles by HCMEC D3 (top) and RAW 246.7 (bottom) cells.